Microstructural and thermomechanical simulation of the additive manufacturing process in 316L austenitic stainless steel

M.P. Sotiriou[1], J.S. Aristeidakis[1], M.I.T. Tzini[1], I. Papadioti[1], G.N. Haidemenopoulos[1] and N. Aravas[1,2]

[1] Department of Mechanical Engineering, University of Thessaly, Volos, Greece
[2] International Institute for Carbon Neutral Energy Research (WPI-I2CNER), Kyushu University, 744 Motooka, Nishi-ku, Fukuoka 819-0395, Japan

IEC2M 2021

The 1st International Electronic Conference on Metallurgy and Metals

22 FEBRUARY – 07 MARCH | ONLINE

Introduction to Additive Manufacturing Modeling

Additive Manufacturing (AM)
Laser Powder Bed Fusion

Temperature Gradient

Microstructural phenomena
Solidification
Solid-state transformations

Microsegregation
Freezing range

Mechanical phenomena
Elastic and Plastic deformation

Residual stresses
Mechanical properties

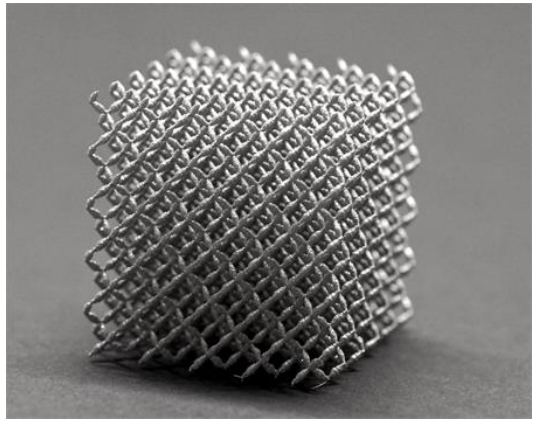

Image source: 3dprint.com

Image source: 3Druck.com

Project Objective: Development of an **integrated** thermomechanical and microstructural model

Microstructural and Thermomechanical Coupling

316L Composition: 18Cr-14Ni-2.6Mo-0.03C-1Mn (wt%)

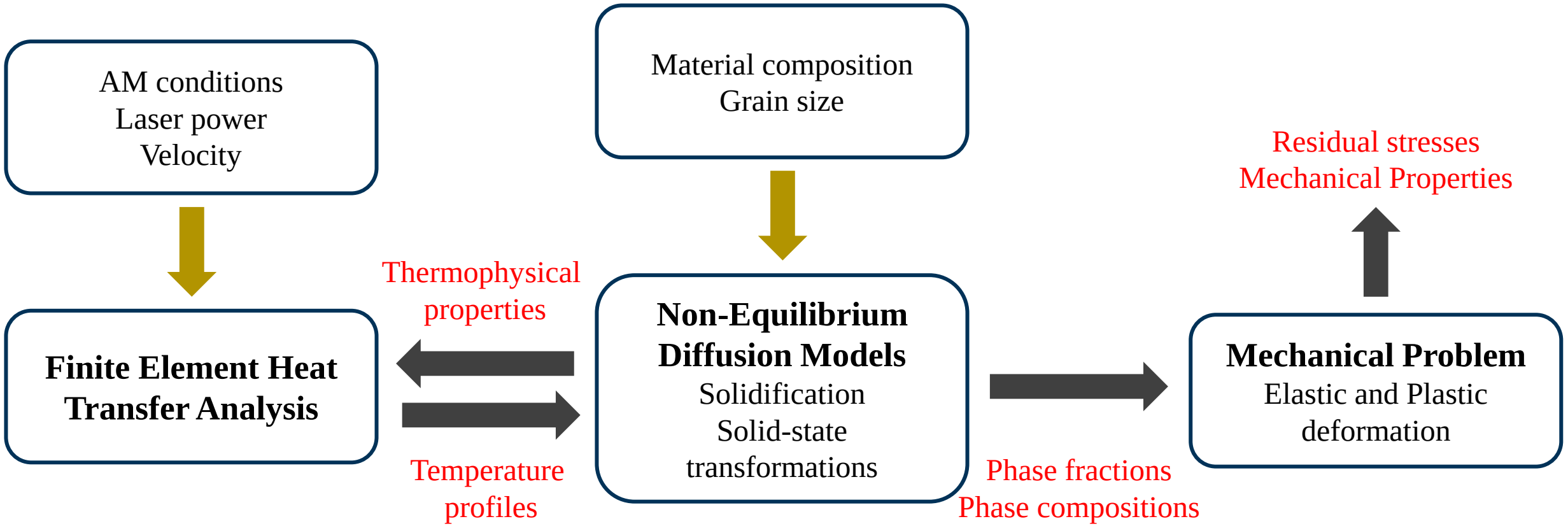

Heat Transfer Analysis

ABAQUS: FEM Analysis

- Energy balance, constitutive equations
- Latent heat, convection and radiation
- Quiet element method [1] $k_{quiet} = c_{quiet} = 0$
- Heat input model: Double ellipsoid volumetric source heat input [2] $P = 195$ W, $v = 20$ mm/s, idle time $= 10$s

Material data: $U_{latent} = 330 \frac{kJ}{kg}, \rho = 8030 \frac{kg}{m^3}$

Temperature (°C)	26.85	636.85	1226.85	2126.85
Thermal conductivity k (W/m/°C)	13.9	23.3	32.8	19.6
Specific heat c (kJ/kg/°C)	0.498	0.578	0.658	0.769

Boundary conditions: $h = 30 \frac{\mathrm{W}}{\mathrm{m}^2\,^{\circ}\mathrm{C}}$, $H = 630 \frac{\mathrm{W}}{\mathrm{m}^2\,^{\circ}\mathrm{C}}$, $\varepsilon = 0.5$, $T_0 = 27\,^{\circ}\mathrm{C}$

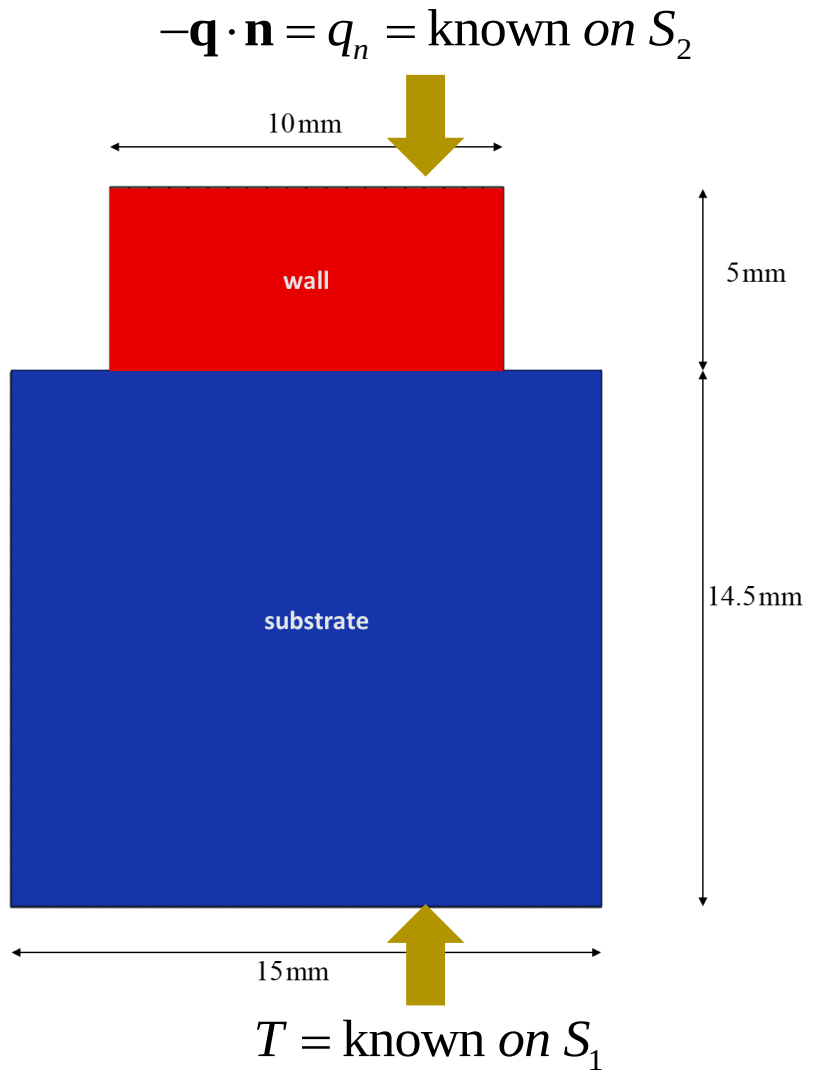

[1] Michaleris, P. Modeling metal deposition in heat transfer analyses of additive manufacturing processes. *Finite Elem. Anal. Des.* **2014**, *86*, 51–60, doi:10.1016/j.finel.2014.04.003.
[2] Goldak, J.; Chakravarti, A.; Bibby, M. A new finite element model for welding heat sources. *Metall. Trans. B* **1984**, *15*, 299–305, doi:10.1007/BF02667333.

Microstructural Analysis

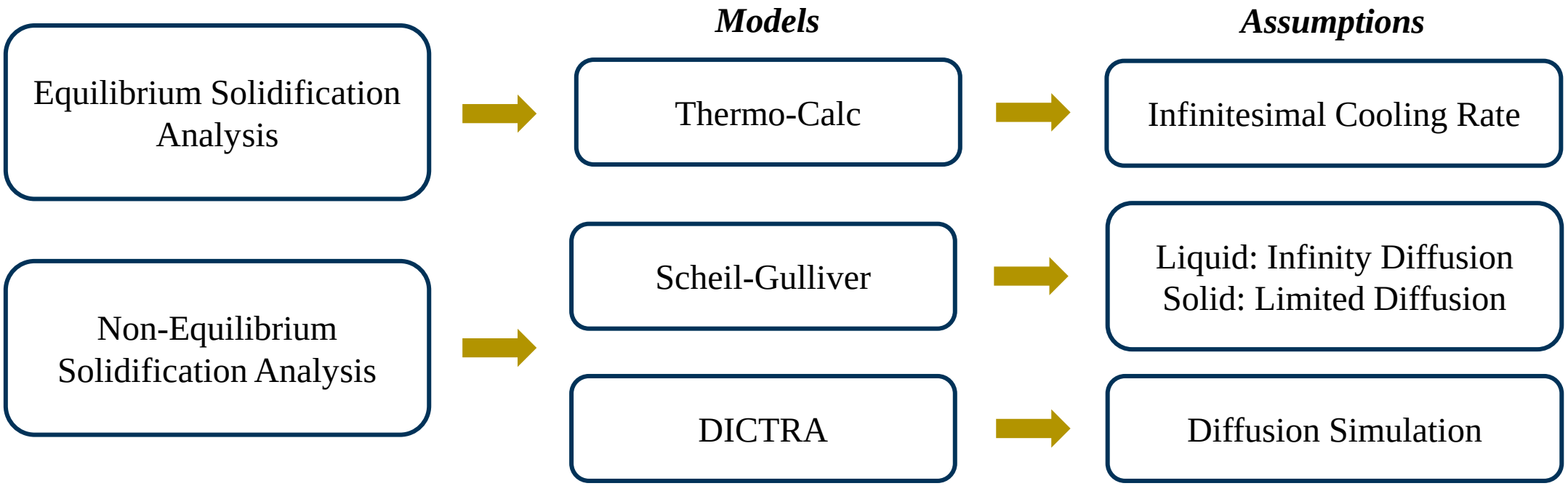

DICTRA Eutectic ALF refers to γ/L/δ

$$L \rightarrow \gamma + \delta$$

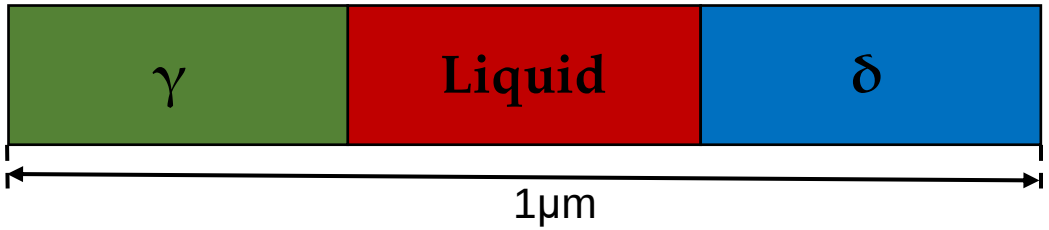

Temperature History Plots

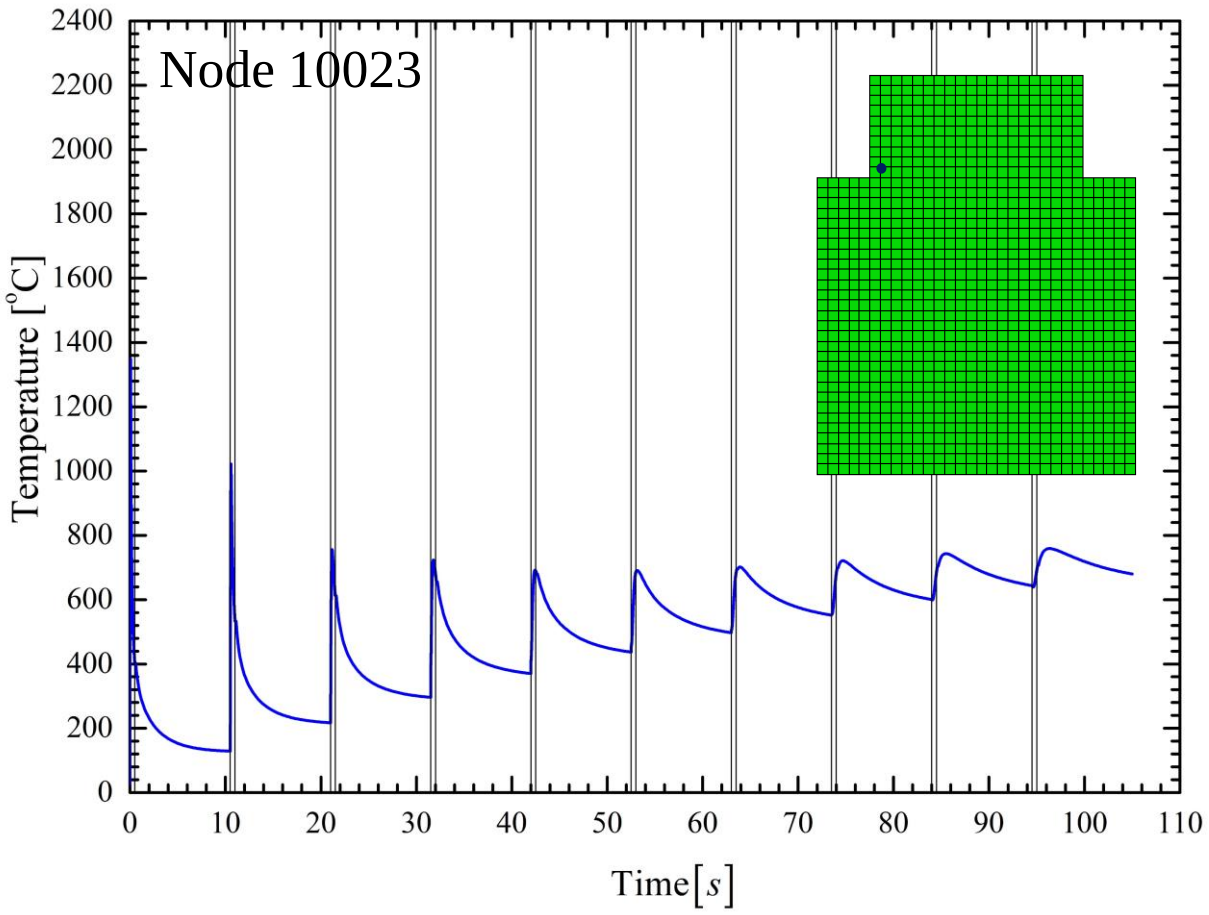

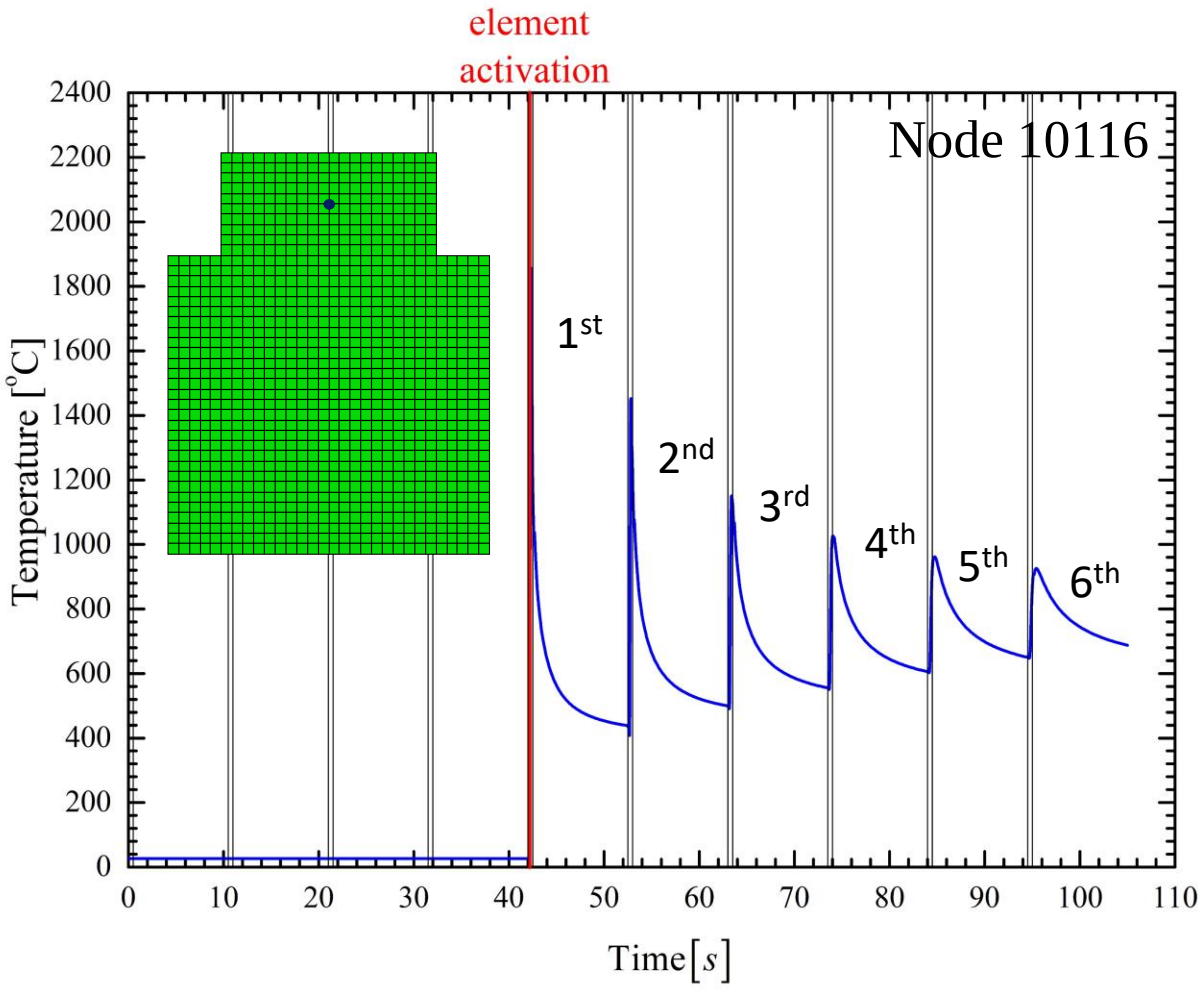

Equilibrium Solidification

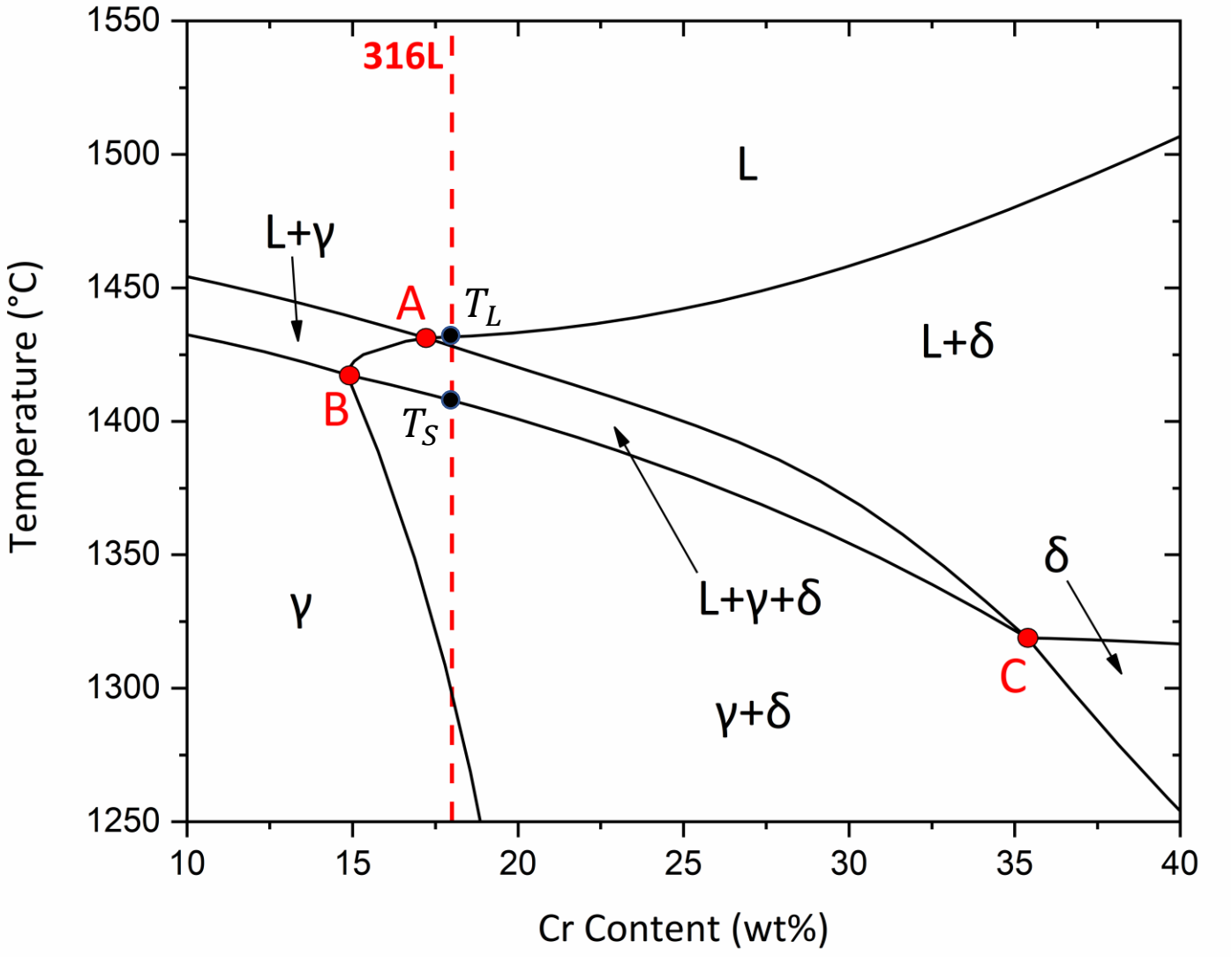

Solidification Type

Ferritic-Austenitic

$$L \rightarrow \delta + L \rightarrow \gamma + \delta + L \rightarrow \gamma + \delta$$

Freezing range: $T_L - T_S$ = **21.3°C**

Note: Sensitive to carbon (C) concentration

Solidification model comparison

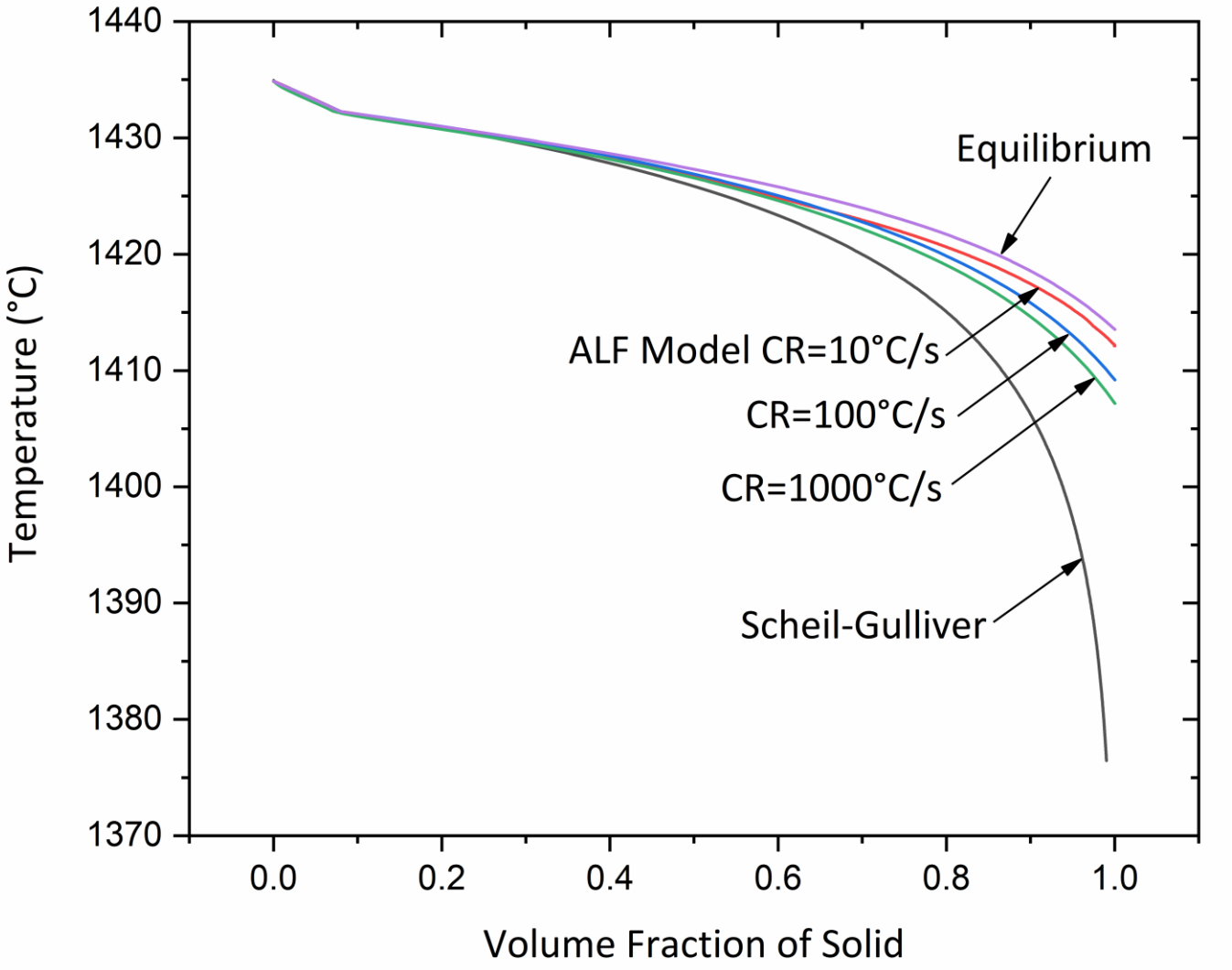

Low limit case
Equilibrium

ALF DICTRA

Cooling rate increases

Sluggish diffusion kinetics

Scheil-Gulliver
High limit case

Evolution of Phase Fractions

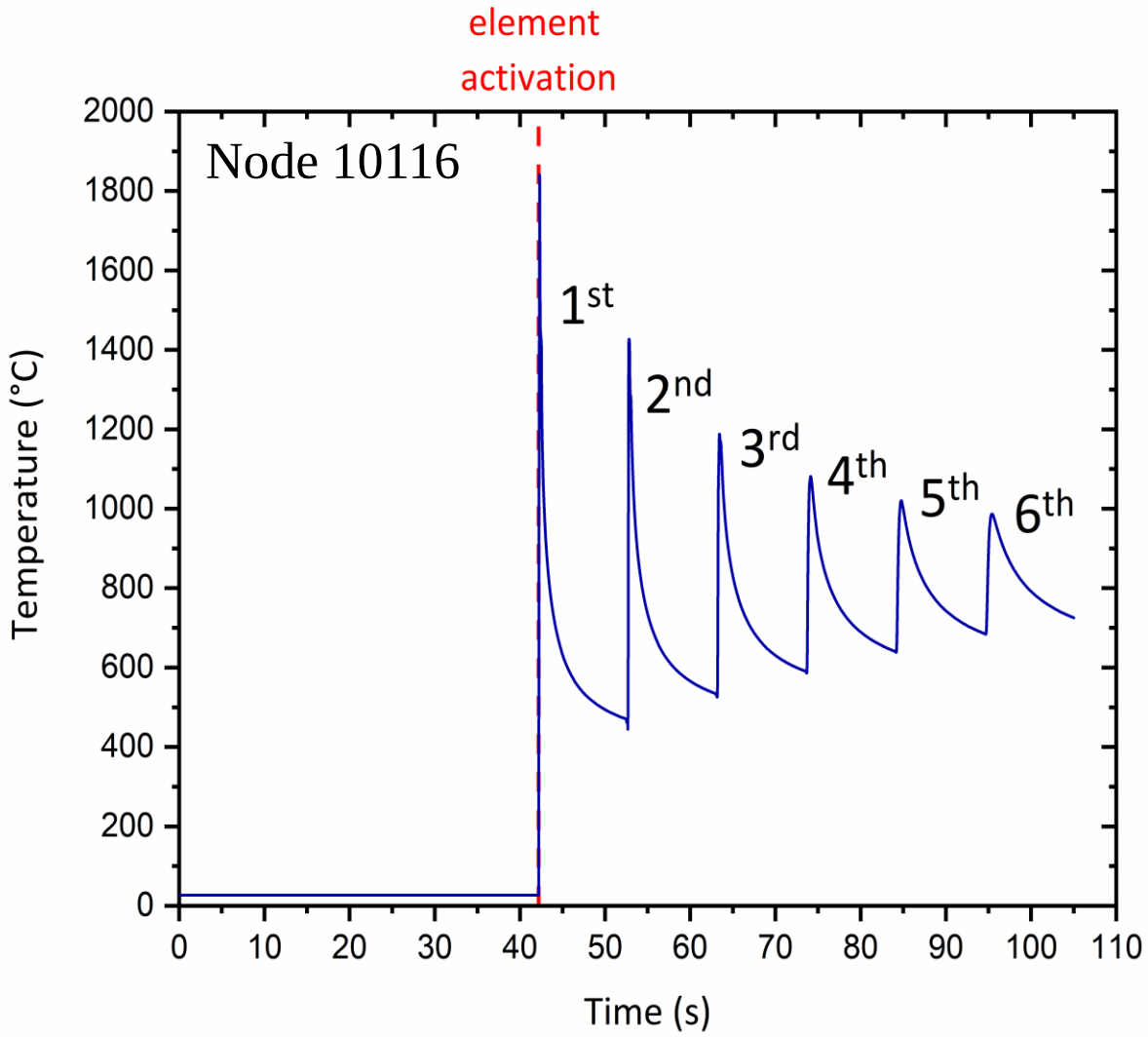

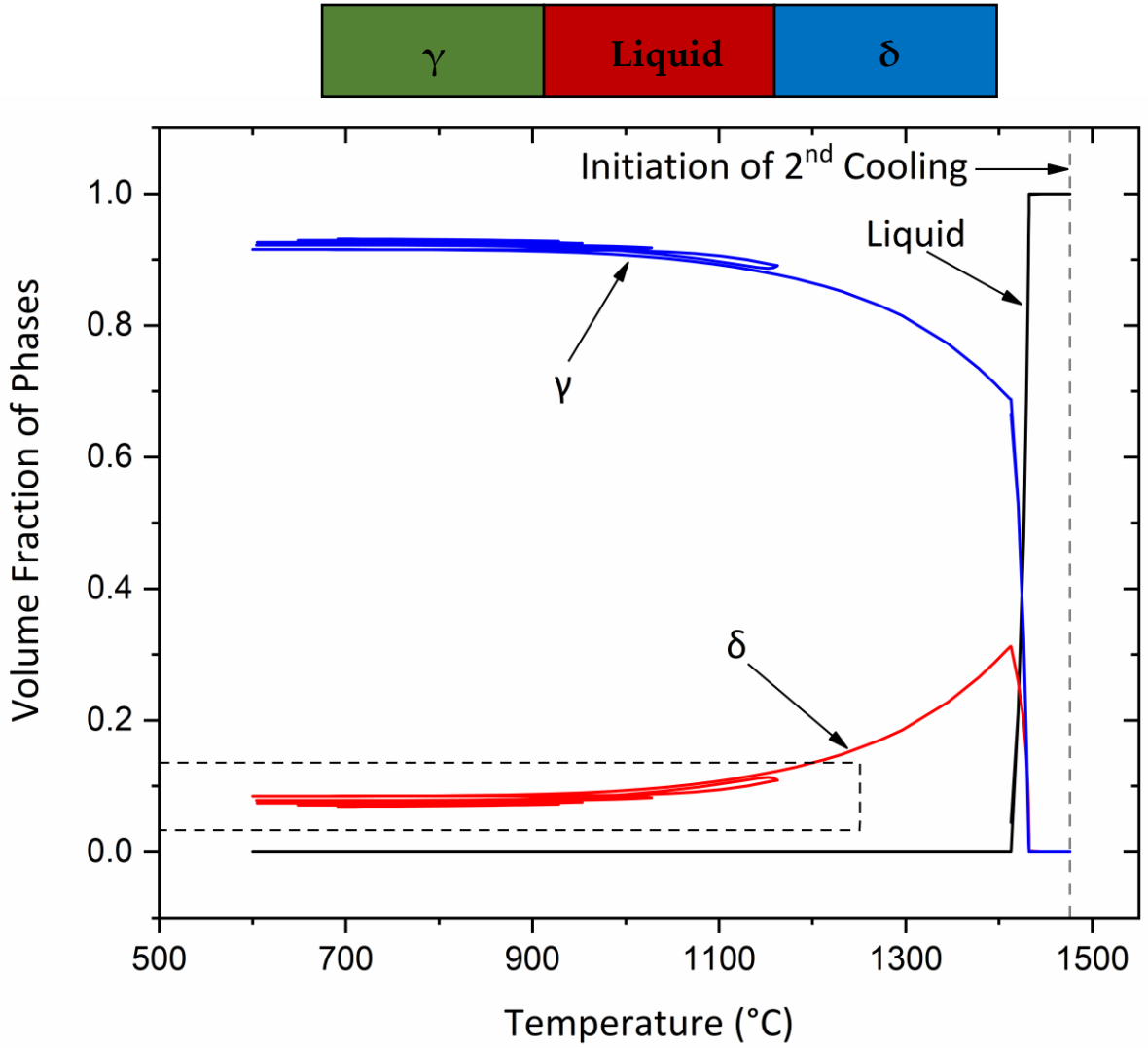

Evolution of δ-Fe during Thermal Cycling

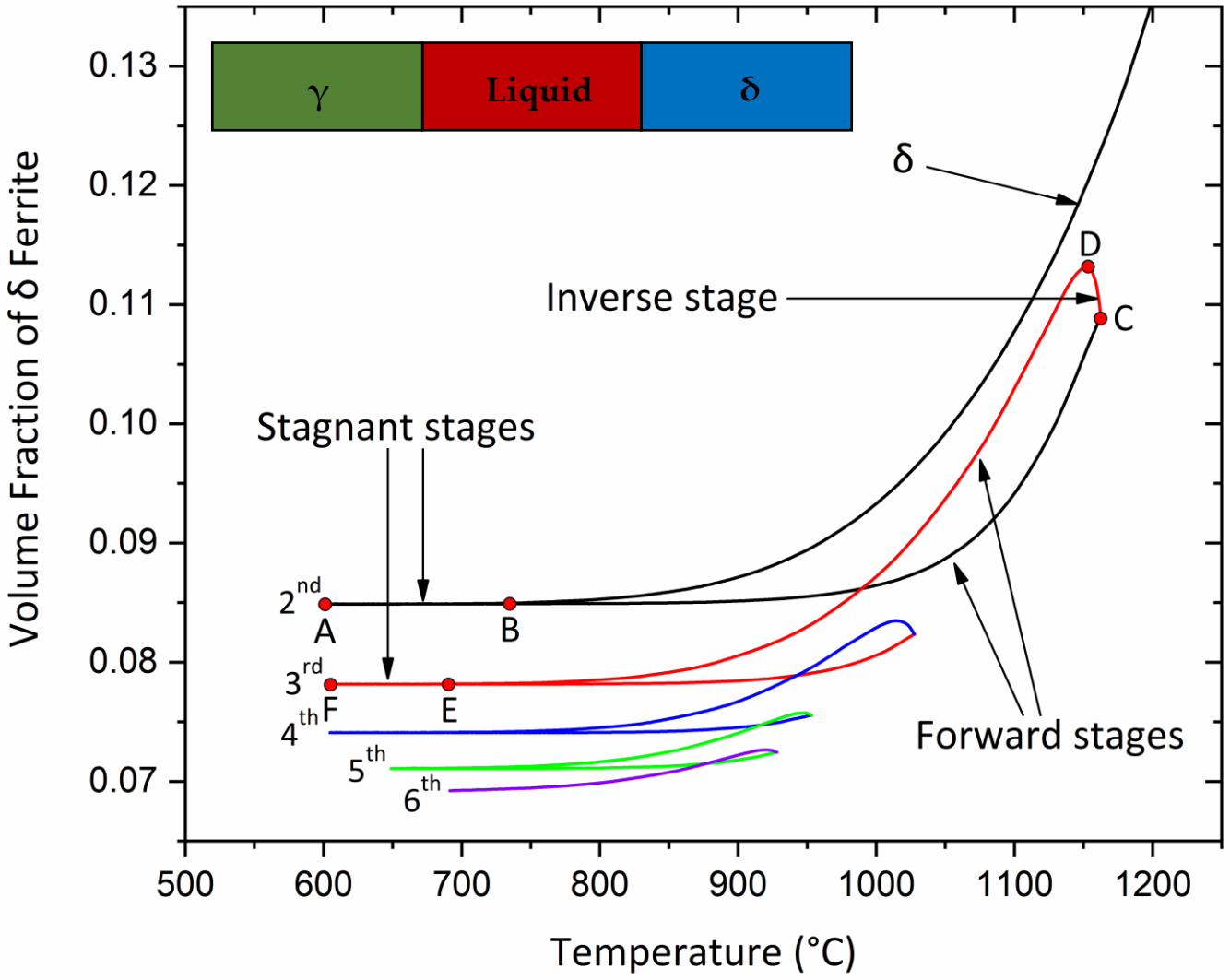

Evolution of Phase Concentrations

Final segregation profiles

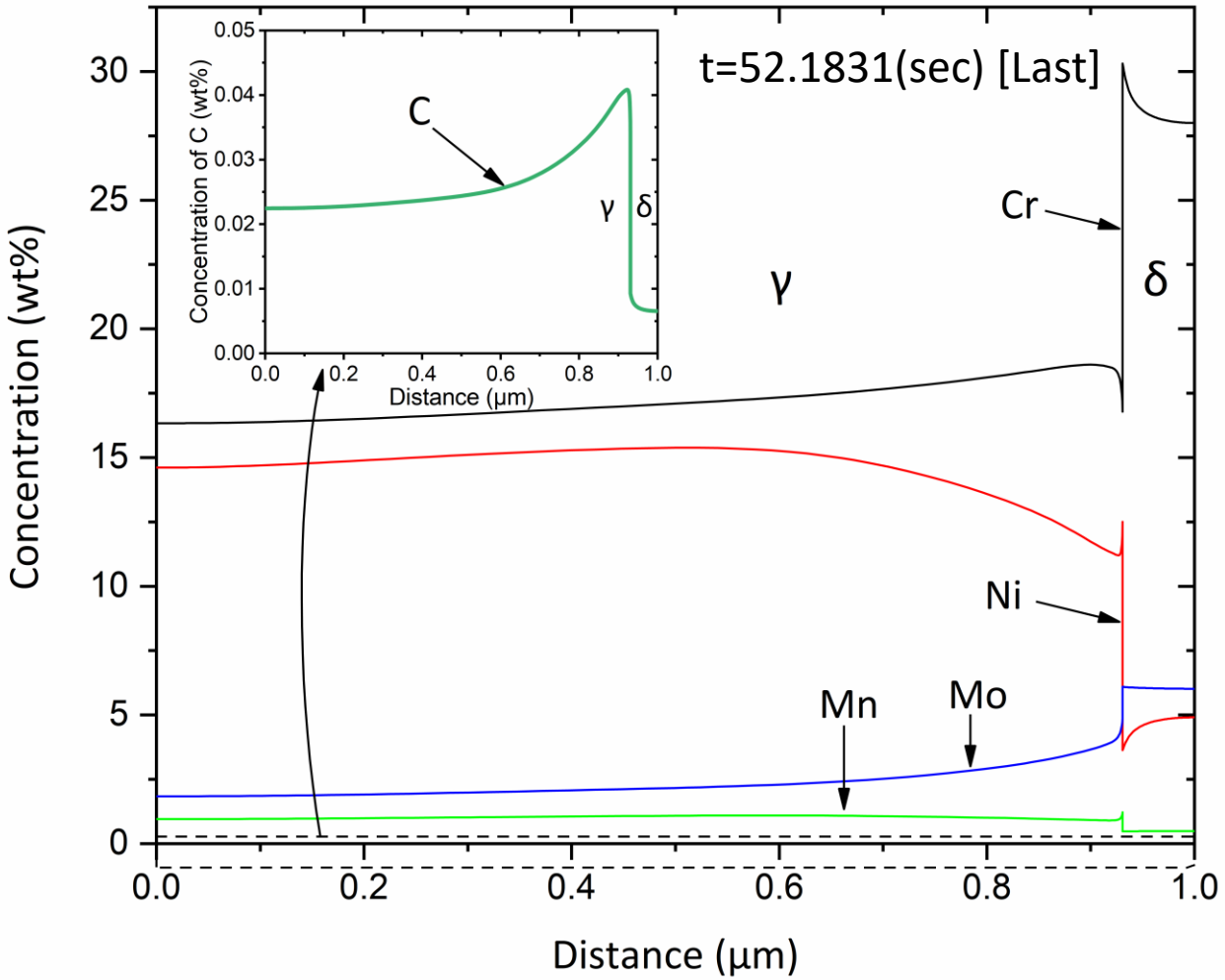

Cr, Ni microsegregation after each cooling

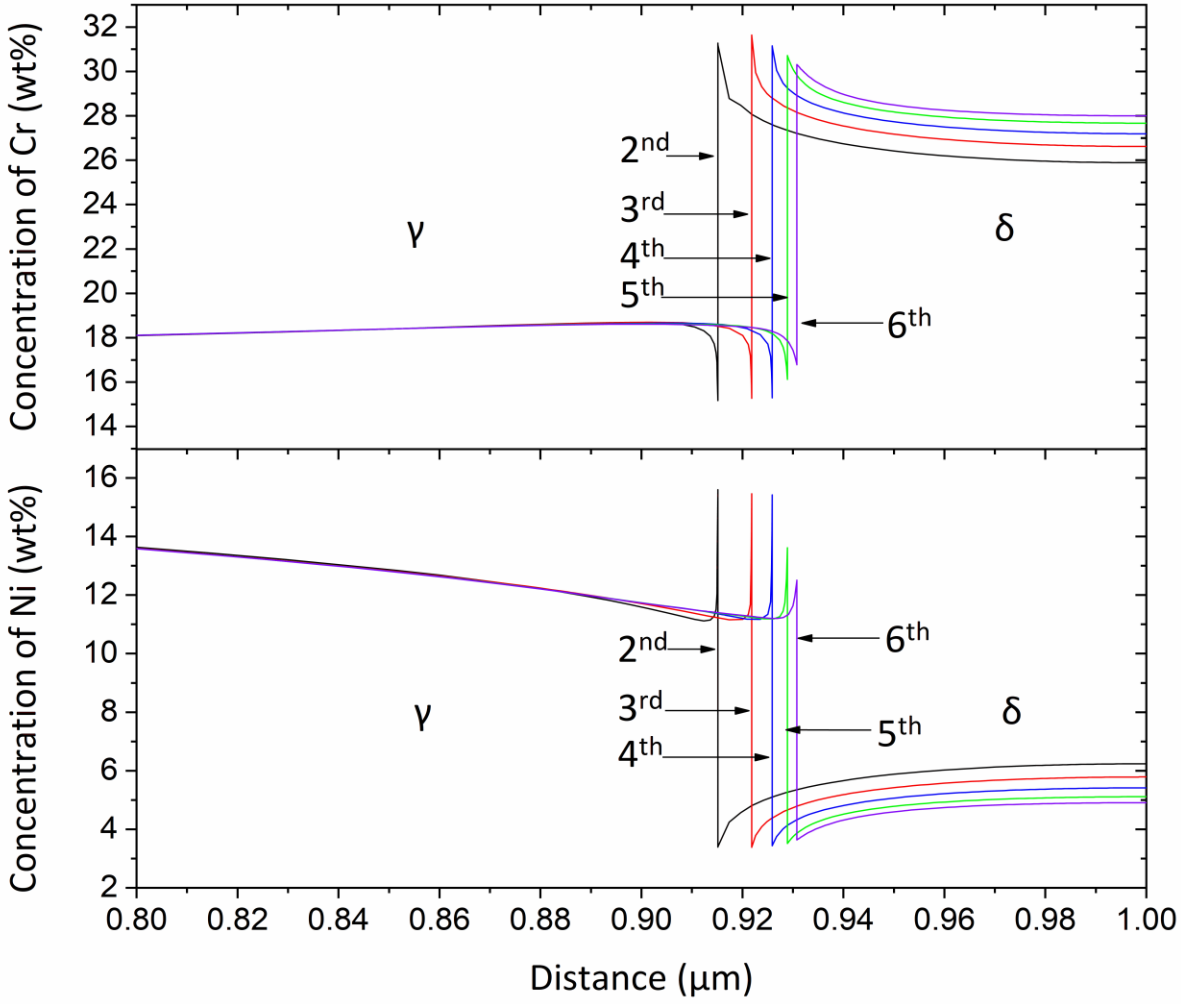

Conclusions

Thermal history → Microstructural evolution

Key parameter for solidification → Diffusion kinetics

Processing parameters (e.g., Cooling rate) →
- Freezing range
- Cr & Ni Segregation

Thermal cycling effect → Microsegregation decrease

Phase fractions and constitutions can be provided as input for the mechanical analysis to calculate the residual stresses and distortions

Thank you for your attention!

Image source: GE